MOLECULAR ONCOLOGY 9 (2015) 1406–1420

available at www.sciencedirect.com

ScienceDirect

www.elsevier.com/locate/molonc

Natural product (−)-gossypol inhibits colon cancer cell growth by targeting RNA-binding protein Musashi-1

Lan Lan[a], Carl Appelman[a], Amber R. Smith[a], Jia Yu[a,j], Sarah Larsen[a], Rebecca T. Marquez[a], Hao Liu[a,1], Xiaoqing Wu[a], Philip Gao[b], Anuradha Roy[c], Asokan Anbanandam[d], Ragul Gowthaman[a,e], John Karanicolas[a,e], Roberto N. De Guzman[a], Steven Rogers[f], Jeffrey Aubé[f,g,h,i], Min Ji[j], Robert S. Cohen[k], Kristi L. Neufeld[a], Liang Xu[a,m,*]

[a]Department of Molecular Biosciences, The University of Kansas, Lawrence, KS, USA
[b]COBRE Protein Production Group, The University of Kansas, Lawrence, KS, USA
[c]High Throughput Screening Laboratory, The University of Kansas, Lawrence, KS, USA
[d]Bio-NMR Core Facility, The University of Kansas, Lawrence, KS, USA
[e]Center for Bioinformatics, The University of Kansas, Lawrence, KS, USA
[f]Center of Biomedical Research Excellence, Center for Cancer Experimental Therapeutics, The University of Kansas, Lawrence, KS, USA
[g]Specialized Chemistry Center, The University of Kansas, Lawrence, KS, USA
[h]Center for Chemical Methodologies and Library Development, The University of Kansas, Lawrence, KS, USA
[i]Department of Medicinal Chemistry, The University of Kansas, Lawrence, KS, USA
[j]School of Chemistry and Chemical Engineering, Southeast University, Nanjing, China
[k]Department of Biological Sciences, Clemson University, Clemson, SC, USA
[m]Department of Radiation Oncology, The University of Kansas Cancer Center, Kansas City, KS, USA

ARTICLE INFO

Article history:
Received 30 December 2014
Received in revised form
9 March 2015
Accepted 27 March 2015
Available online 10 April 2015

Keywords:
RNA binding protein
Wnt
Notch
Musashi-1
Colon cancer

ABSTRACT

Musashi-1 (MSI1) is an RNA-binding protein that acts as a translation activator or repressor of target mRNAs. The best-characterized MSI1 target is *Numb* mRNA, whose encoded protein negatively regulates Notch signaling. Additional MSI1 targets include the mRNAs for the tumor suppressor protein APC that regulates Wnt signaling and the cyclin-dependent kinase inhibitor $P21^{WAF-1}$. We hypothesized that increased expression of NUMB, P21 and APC, through inhibition of MSI1 RNA-binding activity might be an effective way to simultaneously downregulate Wnt and Notch signaling, thus blocking the growth of a broad range of cancer cells. We used a fluorescence polarization assay to screen for small molecules that disrupt the binding of MSI1 to its consensus RNA binding site. One of the top hits was (−)-gossypol (Ki = 476 ± 273 nM), a natural product from cottonseed, known to have potent anti-tumor activity and which has recently completed Phase IIb clinical trials for prostate cancer. Surface plasmon resonance and nuclear magnetic resonance studies demonstrate a direct interaction of (−)-gossypol with the RNA binding pocket of MSI1. We further showed that (−)-gossypol reduces Notch/Wnt signaling in several colon cancer cell lines having high levels of MSI1, with reduced *SURVIVIN* expression and

* *Corresponding author*. Department of Molecular Biosciences, University of Kansas, 4002 Haworth Hall, 1200 Sunnyside Avenue, Lawrence, KS 66045-7534, USA. Tel.: +1 785 864 5849; fax: +1 785 864 1442.
E-mail address: xul@ku.edu (L. Xu).
[1] Current address: Key Laboratory of Biomedical Information Engineering of Ministry of Education, School of Life Science and Technology, Xi'an Jiaotong University, Xi'an, China.
http://dx.doi.org/10.1016/j.molonc.2015.03.014

increased apoptosis/autophagy. Finally, we showed that orally administered (−)-gossypol inhibits colon cancer growth in a mouse xenograft model. Our study identifies (−)-gossypol as a potential small molecule inhibitor of MSI1-RNA interaction, and suggests that inhibition of MSI1's RNA binding activity may be an effective anti-cancer strategy.

1. Introduction

Musashi-1 (MSI1) is an evolutionarily conserved protein best known for its role in neural development in invertebrates. Msi1 was first identified in *Drosophila* where it helps establish different levels of Notch signaling in the daughters of a sensory organ progenitor (SOP) cell (Nakamura et al., 1994). Subsequent studies indicate a similar role for Msi1 in the asymmetric divisions of other precursor cells, including *Drosophila* male germline stem cells (Kaneko et al., 2000; Okano et al., 2005; Potten et al., 2003; Siddall et al., 2006). Homologs of *Drosophila* Msi1 have been identified in other species including mouse, *Xenopus* and humans (Charlesworth et al., 2006; Kaneko et al., 2000; Potten et al., 2003; Sakakibara et al., 1996; Sugiyama-Nakagiri et al., 2006; Toda et al., 2001), where the protein is also expressed in stem cells and/or other precursor cell populations. Other MSI1 functions have been identified including a role in microRNA biogenesis (Kawahara et al., 2011). MSI1 is also overexpressed in a variety of human cancers, including glioblastoma, breast, and colon cancers (Fan et al., 2010; Ma et al., 2008; Potten et al., 2003; Seigel et al., 2007; Sureban et al., 2008; Toda et al., 2001; Wang et al., 2010; Ye et al., 2008; Yokota et al., 2004), with the highest levels occurring in late stage cancers (Fan et al., 2010; Li et al., 2011; Sureban et al., 2008; Wang et al., 2010). Taken together, these data indicate that MSI1 is a cell fate determinant that drives cells toward the less differentiated (more proliferative) fate through maintenance of high levels of Notch and/or Wnt signaling (further discussed below). The loss of MSI1 expression from stem cells or other precursor cell populations results in the loss of such cells and a corresponding expansion of differentiated cell populations, while the over-expression of MSI1 leads to the expansion of undifferentiated and a decrease in differentiated cell populations (Okano et al., 2005; Siddall et al., 2006).

Several observations suggest that MSI1 upregulates Notch and Wnt signaling by repressing the translation of *Numb* (Imai et al., 2001; Takahashi et al., 2013) and *APC* (adenomatous polyposis coli) (Spears and Neufeld, 2011), which act as negative regulators of Notch and Wnt signaling, respectively (Moon and Miller, 1997; Pece et al., 2004). MSI1 also represses translation of $P21^{WAF-1}$ (Battelli et al., 2006), a negative regulator of cell cycle progression. MSI1 contains a well-conserved RNA binding domain (RBD) and exhibits sequence-specific RNA binding activity *in vitro* (Battelli et al., 2006; Imai et al., 2001; Spears and Neufeld, 2011). *Numb*, *APC* and *P21* mRNAs each contain at least one copy of the MSI1 consensus RNA binding sequence (MCS) (Battelli et al., 2006; Imai et al., 2001; Spears and Neufeld, 2011), and the direct binding of MSI1 to these sites has been established for both *Numb* and $P21^{WAF-1}$ (Battelli et al., 2006; Imai et al., 2001). In the case of *APC* and *Numb*, deletion of the sites from the 3′-UTRs resulted in increased luciferase expression in luciferase reporter assays (Imai et al., 2001; Spears and Neufeld, 2011).

Post-transcriptional regulation mediated by MSI1 can also be positive. Translational activation activities of MSI1 have been reported in pre-cerebellar neurons during midline crossing (Kuwako et al., 2010) and during *Xenopus* oocyte maturation (Charlesworth et al., 2006).

Our focus is on the function of MSI1 in tumorigenesis and on the development of small molecule inhibitors of MSI1 as a possible novel therapeutic approach. The identification of compounds that specifically interfere with protein–protein interactions is recognized as a challenging task, there is an even more severe lack of compounds that directly disrupt protein–RNA interactions. While previous studies have identified small molecule inhibitors of MSI family proteins, none of these studies measured *in vivo* anti-cancer activities (Clingman et al., 2014; Minuesa et al., 2014). In this work, we use a fluorescence polarization (FP) competition assay to identify (−)-gossypol, a natural product from cottonseed, as a potent inhibitor of MSI1-RNA binding. We further show using surface plasmon resonance (SPR) and nuclear magnetic resonance (NMR) assays that (−)-gossypol binds MSI1 directly, and inhibits Notch and Wnt signaling in a variety of colon cancer cell lines. (−)-Gossypol has completed Phase IIb multicenter clinical trials for treating prostate cancer (e.g., NCT00286806, NCT00286793, NCT00666666) and a variety of other cancers (e.g., NCT00275431, NCT00397293). These clinical trials stemmed from previous work including ours, which showed that (−)-gossypol induces autophagy and apoptosis in prostate and other cancer cell lines through inhibition of the Bcl-2 family of anti-apoptotic proteins (Keshmiri-Neghab and Goliaei, 2014; Lian et al., 2011; Meng et al., 2008; Mohammad et al., 2005; Paoluzzi et al., 2008; Zhang et al., 2003, 2010). Our *in vitro* fluorescent polarization binding assays indicate that (−)-gossypol has a similar or higher affinity for MSI1 ($Ki = 476 \pm 273$ nM) than that of the Bcl-2 family member, BCL-xL ($Ki = \sim 0.48$ μM) (data not shown and US patent 8163805 B2 (Wang et al., 2012)). (−)-Gossypol has a lower affinity to BCL-2 than BCL-xL (IC50 10 μM vs 0.4 μM) in the same experiment condition (Wang et al., 2012; Zhang et al., 2003). This suggests that (−)-gossypol might have value in treating colon and other cancers associated with high levels of MSI1 expression.

2. Materials and methods

2.1. Cell culture and reagents

CCD-841 (normal colon epithelial) and human colon cancer cell lines HCT-116, HT-29, DLD-1 and LS174T were obtained from American Type Culture Collection (ATCC). HCT-116 β/W was provided by Dr. Bert Vogelstein. HCT-116 β/W contains one copy of the wild type β-catenin while β-catenin in HCT-116 is heterozygous mutant (Chan et al., 2002). All cells were maintained in DMEM (Mediatech, Manassas, VA) supplemented with 10% fetal bovine serum (FBS) (Sigma–Aldrich, St. Louis, MO), 1% Glutamine (Mediatech), 1% antibiotics (Mediatech). (−)-Gossypol was isolated from racemic gossypol as we previously described (Lian et al., 2011; Meng et al., 2008). (3, 4-Dimethoxyphenyl) methanimine gossypol (MP-Gr) was synthesized from gossypol (Supplementary Methods). The (−)-Gossypol and MP-Gr powder were dissolved in DMSO at 20 mM as stock solutions. Cell growth, western blot analysis, Caspase-3 activation assay, RT-PCR and quantitative real-time PCR were carried out according to our previous publications (Li et al., 2014, 2013; Lian et al., 2011; Meng et al., 2008; Wu et al., 2010). Primers sequences are listed in Supplementary Table 1. The primary antibodies used were anti-Cyclin D1 (SC-753) and anti-P21 (SC-397, Lot#A1007) (Santa Cruz Biotechnology, Santa Cruz, CA), anti-α-tubulin (T5168) (Sigma, St. Louis, MO), anti-c-Myc (#5605), anti-PARP (#9542), anti-Caspase 3 (#9662), anti-MSI1 (#5663) and anti-Numb (#2756) (Cell Signaling Technology, Danvers, MA), anti-Survivin (NB500-201) (Novus Biologicals, Littleton, CO) and anti-Notch1 (ab8925) (Abcam, Cambridge, UK). The secondary antibodies used were goat-anti-mouse-HRP, goat-anti-rabbit-HRP (Sigma, St. Louis, MO). Bafilomycin A1 used in autophagy assays is from Sigma (Sigma, St. Louis, MO). Western blot band intensities were measured using Image Studio Ver 4.0 (LI-COR Biosciences, Lincoln, NE).

2.2. MTT-based cytotoxicity assay

Cell viability was determined by the MTT-based assay using Cell Proliferation Reagent WST-8 (GenScript, Piscataway, NJ). Cells (4000–5000 cells/well, except WI-38 was 10,000 cells/well) were plated in 96-well culture plates, and serially diluted testing compounds were added to the cells in triplicates. Four to six days later, when DMSO control wells reach confluences, WST-8 was added to each well and incubated for 2 h at 37 °C. Absorbance was measured with Synergy H4 plate reader (Biotek, Winooski, VT) at 450 nm with correction at 650 nm. The results are expressed as the percentage of absorbance of treated wells versus that of DMSO control. IC50, the drug concentration causing 50% growth inhibition, was calculated via sigmoid dose response curve fitting using GraphPad Prism 5.0 (GraphPad, Winooski, VT).

2.3. Colony formation assay

For colony formation assay, cells were seeded in 6-well plate in triplicate (400 cells/well) and treated with (−)-gossypol, MP-Gr at different dose or DMSO control (concentration 0 in both (−)-gossypol and MP-Gr treated samples). 0.5 ml of FBS was added to each well at day 5. After 10 days of incubation, plates were gently rinsed with PBS and stained with 0.1% of crystal violet (in PBS). Colonies with over than 50 cells were counted manually. Survival fraction was calculated by dividing the number of colonies in the treatment group by that of the DMSO control.

2.4. Protein expression and purification

pGEX4T-1-MSI1 and pET21a-GB1-RBD1 plasmids encoding full length MSI1 and the RNA binding domain 1 (RBD1, residues 20–107) of MSI1 were constructed with *Mus musculus* cDNAs under Tac and T7 promoter, respectively. The amino acid sequence of RBD1 is identical in *Homo sapiens* and *Mus musculus*. GST-MSI1 and GB1-RBD1 proteins were expressed in *E. coli* and purified as previously described (Estrada et al., 2009; Harper and Speicher, 2011) with modifications for GB1-RBD1 protein production (Supplementary Methods).

2.5. Fluorescence polarization competition assay

The oligonucleotide sequence for MSI1 RNA binding studies was 5′-UAGGUAGUAGUUUUA-3′, corresponding to 2781–2795 of the published *Numb* mRNA sequence (NM_001272055.1) and was previously shown to bind MSI1 (Imai et al., 2001). A 16-nt fully degenerative *control* RNA was used as a negative control. *Control* RNA is a mixture of 16-nt oligos with random sequences. The 3′-fluorescein-labeled *Numb* and *control* RNAs were purchased from Dharmacon (Thermo Scientific, Lafayette, CO) and deprotected as recommended by the manufacturer. Unlabeled versions of the *Numb* and *control* RNAs, used in RNA competition assays, were purchased from IDT (Coralville, IA). FP assays were carried out according to previous publications with our modification (Aviv et al., 2003; Pagano et al., 2011). Briefly, before binding analysis, RNAs were heated to 95 °C for 5 min and immediately cooled on ice for 5 min. For the determination of equilibrium dissociation constants (Kd), purified proteins were serially diluted in binding buffer containing 150 mM NaCl, 20 mM HEPES, pH 7.4, 1 mM DTT, 0.05% pluronic F-68, and aliquoted to 96-well assay plates (Corning 3915) (Corning, Corning, NY). For binding reactions, 2 nM of fluorescein-labeled RNA was added to each well and incubated at room temperature for 30 min. Anisotropy measurements were taken at room temperature using a BioTek Synergy H4 plate reader (Biotek, Winooski, VT) following the protocol recommended by the manufacture. The Kd was estimated by nonlinear regression to a one-site binding model using GraphPad Prism 5.0 (GraphPad, San Diego, CA). For RNA competition assays, increasing concentrations of unlabeled *Numb* or *control* RNAs were added to pre-formed *Numb* RNA-protein complexes. For the drug screening/competition assay, different testing compounds with single (10 μM) or multiple concentrations (6 doses ranging from 2 nM to 200 μM) were added to each well prior to the addition of the *Numb* RNA-protein complexes. After 2 h of incubation at room temperature, anisotropy measurements were taken. IC50, the drug concentration causing 50% inhibition, was calculated via sigmoid dose response curve fitting using

Prism 5.0. Ki value was calculated using free online software (http://sw16.im.med.umich.edu/software/calc_ki/). The percent of inhibition was normalized such that the FP value of the protein-RNA complex with DMSO was defined as 0% inhibition, while the FP value obtained with the same concentration of the free RNA alone was defined as 100% inhibition.

2.6. Surface plasmon resonance (SPR)

The SPR experiments were performed using a BIACORE 3000 (GE Healthcare, Little Chalfont, UK) equipped with a CM5 sensor chip. GB1-RBD1 protein was immobilized using amine-coupling chemistry (Supplementary Methods). For drug studies, test compounds were dissolved in 20 mM HEPES, 1 mM DTT, 100 mM NaCl, 0.05% Pluronic F-68, 5% DMSO, and pH 7.4, and passed over the flow cells in duplicate at concentrations ranging from 2.5 μM to 50 μM at a rate of 30 μl/min at 20 °C. Reaction complexes were allowed to associate and dissociate for 160 seconds each. The surfaces were regenerated with a 10-second injection of 10 mM glycine (pH 3.0, 0.2% SDS). The curves were calculated from the experimentally observed curves by successive subtractions of signals obtained for the reference surface and signals for the running buffer injected under the same conditions as testing compound.

2.7. Nuclear magnetic resonance (NMR)

For NMR analyses, ^{15}N-labeled GB1-RBD1 protein was produced as previously described (Estrada et al., 2009). The MSI1 target RNA sequence used for NMR studies was purchased from IDT. This RNA oligomer (GUAGU) was previously discovered to be the minimal sequence required for MSI1 recognition and binding (Ohyama et al., 2012). The ^{15}N-labeled GB1-RBD1 was prepared at the concentration of 200 μM in NMR buffer (50 mM sodium phosphate pH 7.0, 100 mM NaCl, 10 mM β-mercaptoethanol and 10% D_2O). Labeled GB1-RBD1 was titrated with increasing amounts of (−)-gossypol to obtain molar protein:drug ratios of 1:0, 1:0.5, 1:1, and 1:2. 2D-^{1}H-^{15}N HSQC spectra were recorded for each titration at 298 K on a Bruker Avance 800 MHz NMR instrument, equipped with a triple resonance (^{1}H/^{13}C/^{15}N) cryoprobe. NMR backbone assignments for MSI1-RBD1 were obtained from the BMRB (entry 11450). Data was processed using NMRPipe (Frank Delaglio et al., 1995) and analyzed with NMRView (Johnson, 2004).

2.8. Computational modeling

The model of (−)-gossypol bound to MSI1, was built from the three-dimensional structure of RBD1 in complex with RNA (PDB: 2RS2) (Ohyama et al., 2012). We first built the structure of gossypol and its hydrated aldehyde forms using Open Babel (O'Boyle et al., 2011). We built structures of gossypol in fully hydrated form, partially hydrated form and without hydrate. The AutoDock tools from the MGL software package were used to perform molecular docking studies (Morris et al., 2009). AutoDock implements a Lamarckian genetic algorithm to search the conformational space of the ligand. The grid box was fixed in the RBD1 region centered on the residue F23 with box size set as 40 Å × 44 Å × 56 Å. We performed 200 runs of separate docking for each of the gossypol and its hydrated forms. The final docked conformation was taken to be that with the lowest energy. (−)-Gossypol in its partially hydrated form is found to be the best docked model in complex with MSI1.

2.9. Wnt luciferase reporter assay

HCT-116 cells were plated at a density of 8×10^5 cells per well in a 6-well dish the day prior to transfection. Cells were transfected with 1.6 μg of either TOPFLASH or FOPFLASH reporter constructs and a pRL-TK Renilla luciferase plasmid to control for transfection efficiency and cell number. The pRL-TK vector contains the herpes simplex virus thymidine kinase promoter to provide low to moderate levels of Renilla luciferase expression for normalization. Transfections were performed with Lipofectamine 2000 (Life technologies) according to the manufacturer's instructions. 16 hours after transfection, cells were trypsinized and plated at a density of 8×10^4 cells per well in a 48-well dish. Once cells had attached, cells were stimulated with 20 mM LiCl and treated with individual compounds or DMSO control. Cells were harvested and assayed using the Dual-Glo Luciferase Assay (Promega, Fitchburg, WI) 24 hours after treatment. All firefly luciferase values were normalized to Renilla control.

2.10. Animal studies

In vivo experiments were carried out with 5- to 6-week-old female NCr-nu/nu nude mice purchased from the Harlan laboratory (Indianapolis, IN). Mice were inoculated subcutaneously with 0.2 ml HCT-116 cell suspension (1.5×10^6 cells) using a sterile 23-gauge needle on both sides of the mice. When tumors reached 30 mm^3, the mice were randomized into two groups with 5 mice per group. Group 1 was given 0.05% carboxymethyl cellulose (CMC) as vehicle control; Group 2 was given 10 mg/kg (−)-gossypol in 0.05% CMC. Both vehicle control and drug were administrated by oral gavage daily for 4 weeks. The tumor sizes and animal body weights were measured twice weekly and plotted according to our published methods (Lian et al., 2011). Briefly, the tumor sizes were measured using vernier caliper, and tumor volume were calculated using formula ½(Length × Width^2) (Lian et al., 2011). One week after treatment, tumor tissues were excised and processed for western blot analysis as we previously described (Lian et al., 2011). All animal experiments were carried out according to the protocol approved by the University of Kansas Guidelines for Use and Care of Animals.

2.11. Statistical analysis

Using Prism 5.0 software (GraphPad Prism), one-way ANOVA and *t*-Test were used to analyze the *in vitro* data, two-way ANOVA was used to analyze the *in vivo* data. A threshold of $P < 0.05$ was defined as statistically significant.

3. Results

3.1. FP assay identified (−)-gossypol as a potent MSI1-RNA interaction inhibitor

We used a high-throughput, FP-based assay to screen chemical libraries of small molecules for those that disrupt the binding of MSI1 to a synthetic copy of a well-characterized MSI1 binding site located in the 3′-UTR of *Numb* mRNA (5′-UAGGUAGUAGUUUUA-3′) (Imai et al., 2001). In preliminary studies, we found that both full-length MSI1 and a truncated version of the protein consisting of RBD1 only bound to *Numb* RNA and not to a control RNA of random sequences (Figure 1A), therefore demonstrating specificity of the assay. We also found that unlabeled *Numb* RNA could displace the labeled *Numb* RNA, while unlabeled control RNA did not (data not shown). We next screened ~2000 compounds from NCI (Diversity Set II, natural product set and approved oncology drugs) and in-house libraries using full-length MSI1 and ranked them by percent of inhibition (Figure 1B). Several molecules, including (−)-gossypol, inhibited MSI1 binding by more than 80%. We chose (−)-gossypol for further studies since it also scored well in cell-based assays (see below), while other molecules including (+)-gossypol did not (data not shown).

Next, we carried out dose–response experiments using (−)-gossypol and several gossypol Schiff base analogs. As shown in Figure 1C, (−)-gossypol inhibits MSI1 RNA binding at submicromolar Ki values, while the MP-Gr, a biologically inert gossypol analog sharing the similar scaffold, did not inhibit MSI1-RNA binding (Figure 1D). This inhibition was confirmed using the truncated version of the MSI1 protein that only contained RBD1 (Figure 1C).

3.2. SPR and NMR validation of (−)-gossypol binding to MSI1

To confirm the binding of (−)-gossypol to MSI1, we carried out an SPR-based binding assay. As shown in Figure 2A, the SPR assay showed that (−)-gossypol binds to MSI1 RBD1 in a dose-dependent manner. SPR data support that (−)-gossypol interacts with MSI1 by directly binding to MSI1 protein RBD1.

To further confirm the binding of (−)-gossypol to MSI1 and to determine if this binding event affects the RNA binding residues, we employed an NMR assay. First, we reproduced the previously published spectra data for ^{15}N-MSI1-RBD1 bound to a synthetic RNA corresponding to the MSI1 consensus target site (GUAGU) with consistent results, as shown in Figure 2B left panel (Miyanoiri et al., 2003). We identified known RNA binding residues W29, K93, F23 and F65 (Figure 2B right panel), consistent with published peak assignments of MSI1 (Ohyama et al., 2012). Specifically, residue F65 is required for MSI1-RBD1 to bind to target RNA (Imai et al., 2001). In response to increasing doses of (−)-gossypol, residues W29, K93, F23 and F65 peaks exhibited line-broadening, as shown in Figure 2C, suggesting that the compound bound most closely to these residues. Thus (−)-gossypol interacts with the same binding pocket that MSI1 uses to bind target RNA. As described in the Methods section above, *in silico* analysis confirms a feasible binding mode for (−)-gossypol in the lower portion of the RBD1 binding pocket, with aromatic stacking interactions that mimic the cognate RNA and include three of the four shifted residues (F23, K93, F65; Figure 2C right panel). Based on the NMR line-broadening of the remote position W29, (−)-gossypol (see insert in Figure 2C) may also bind to more than one region of the protein or induce a conformational change upon binding.

3.3. (−)-Gossypol inhibits cell proliferation, and induces apoptosis and autophagy in colon cancer cell lines

We measured MSI1 expression in human colon cancer lines and a human epithelial cell line derived from normal colon, CCD-841. As shown in Figure 3A, all of the tested colon cancer cell lines have high levels of *MSI1* mRNA as compared to the control normal cell line, some of them have high levels of MSI1 protein (see Figure 3A, bottom panel Western blot). It is noteworthy that all three bands in the Western blot are MSI1 protein, confirmed by MSI1 siRNA (data not shown). We next analyzed the effects of (−)-gossypol on the growth of colon cancer cell lines with high MSI1 expression. As measured by the MTT-based cell viability assay, (−)-gossypol inhibited the viability of colon cancer cells at a lower concentration compared to the normal control CCD-841 cells (Figure 3B). Decrease in cancer and normal cell viability was measured following treatment with the biological inert analog of (−)-gossypol, MP-Gr, at a slightly higher concentration. From our *in vitro* biophysical binding data (Figure 1C), the binding affinity of MP-Gr (Ki > 200 μM) is more than 200 fold weaker than (−)-gossypol (Ki = 0.476 ± 0.273 μM). In *in vitro* MTT-based cytotoxicity assay, IC50 (HCT-116) was 35.5 μM for MP-Gr versus 8.8 μM for (−)-gossypol (Figure 3B). Similar results were observed for other cell lines (Figure 3B). Consistent with these findings, at the 72 h time point, (−)-gossypol, but not the negative analog MP-Gr, inhibited cell proliferation of the three colon cancer cell lines tested in a cell growth assay (Figure 3C). MP-Gr showed some growth inhibition at the 96 h point. The weak activity of MP-Gr observed may be due to other non-specific targets. Similar to the growth inhibition, (−)-gossypol-treated cancer cells formed fewer colonies, as compared with the MP-Gr-treated cells ($P < 0.01$, n = 3) (Figure 3D, Supplementary Figure 1). Our results indicate a ~4-fold selectivity in active versus negative compounds in cancer cells with high MSI1, while they are not active in normal cells with low MSI1 (all IC50s > 40 μM) (Figure 3B).

Previous studies have demonstrated that gossypol induces apoptosis and/or autophagy in various cancer cell lines with high levels of Bcl-2/Bcl-xL (Lian et al., 2011; Meng et al., 2008; Zhang et al., 2003). To determine whether (−)-gossypol induces apoptosis and autophagy in the colon cancer cell lines with high MSI1, we first measured caspase-3 and PARP cleavage levels with and without treatment of (−)-gossypol. As shown in Figure 4A–B, (−)-gossypol induced caspase-3 activation and PARP cleavage in HCT-116 and DLD-1 cells with high MSI1 levels in a dose-dependent manner. (−)-Gossypol also caused an increase in sub-G1 population in HCT-116 cell (Supplementary Figure 2) and

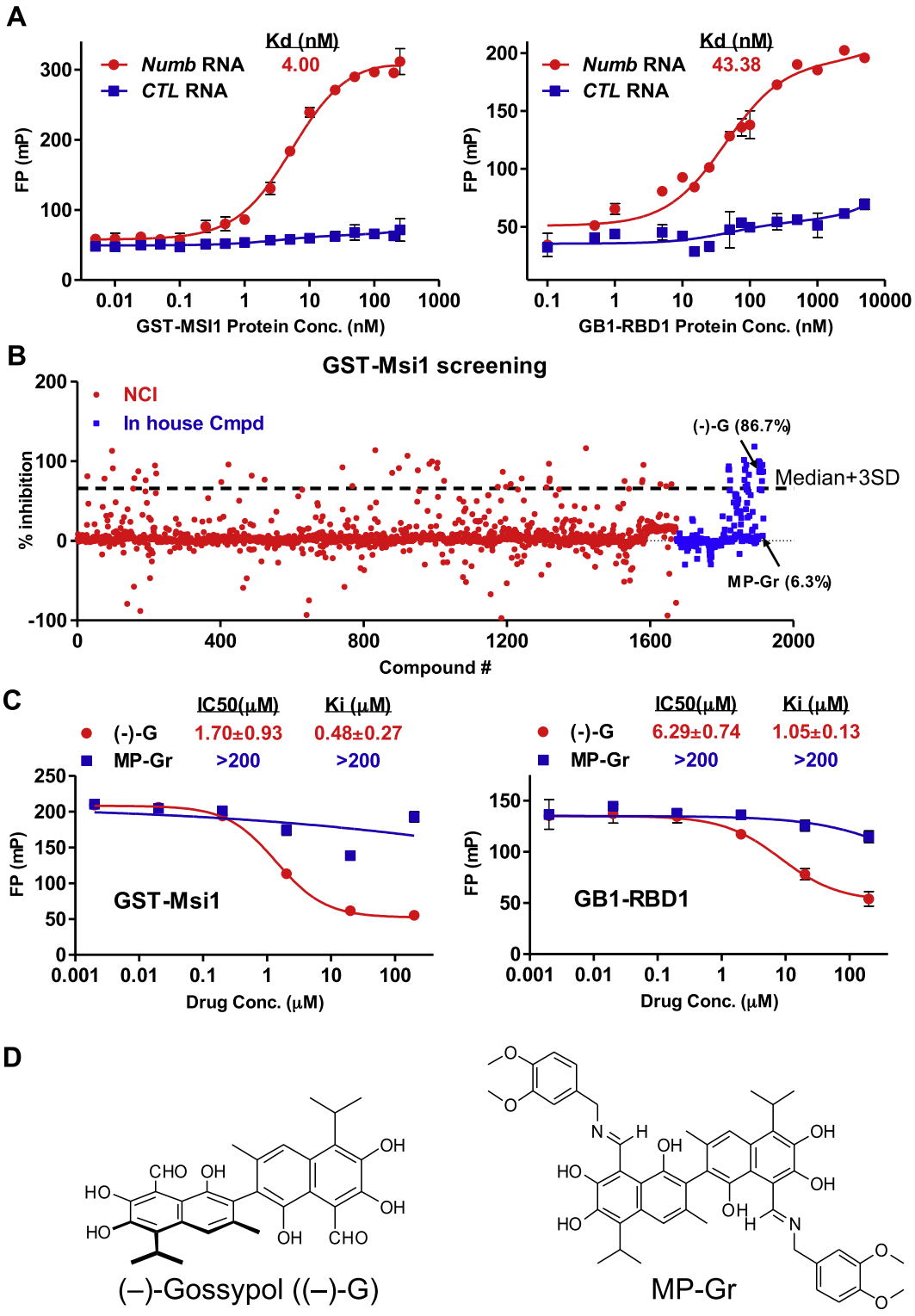

Figure 1 – (−)-Gossypol was identified as a potential MSI1 inhibitor through an initial FP-based drug screening. A. Binding between full length MSI1 (GST-MSI1, left) and RNA binding domain 1 (aa 20–107) of MSI1 (GB1-RBD1, right) to *Numb* RNA. GST-tagged wild-type full length MSI1 (GST-MSI1) or GB1-tagged RBD1 (GB1-RBD1) binds to *Numb*-FITC RNA (5′-UAGGUAGUAGUUUUA-FITC-3′), but not to control oligo-FITC (*CTL* RNA). The concentration of FITC tagged-RNA used in the assay is 2 nM. (n > 3) B. Scattergram of the screening compounds. MSI1/*Numb* mRNA FP-based screening assay was carried out with ~2000 compounds from NCI (Diversity Set II, natural product set and approved oncology drugs) and in-house libraries. Median+3SD was used as a threshold to pick the hits. C. Dose–response curves of the selected hit (−)-gossypol ((−)-G) and its negative analog MP-Gr. Ki values were calculated based on the Kd and the dose–response curves. D. Structure of (−)-gossypol and MP-Gr.

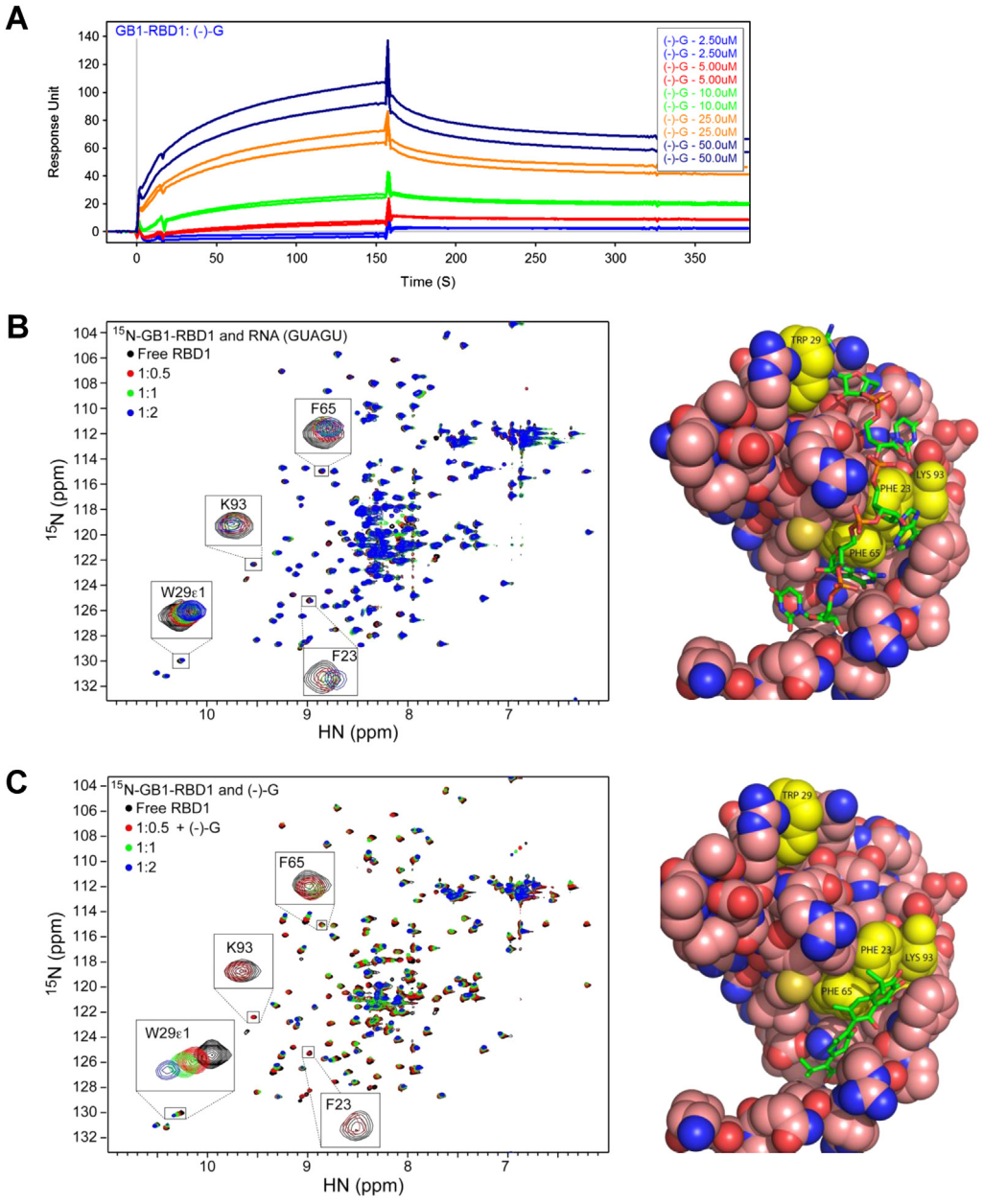

Figure 2 – Validation of (−)-gossypol binding to RBD1 of MSI1. A. SPR analyses of (−)-gossypol binding to immobilized GB1-RBD1. Sensorgram representing direct binding kinetics for (−)-gossypol are shown in response units (RUs) as a function of time (seconds) with increasing concentrations (shown as colorful lines). B. (Left) Overlay of 2D-HSQC spectra sections of 15N-MSI1-RBD1 (black) titrated with RNA oligo (GUAGU). Four of the MSI1-RBD1 RNA binding residues were identified (highlighted in box) and undergo significant line broadening and peak shifts upon addition of RNA. (Right) The structure of RBD1 of MSI1 bound with RNA (PDB 2RS2). The protein atoms are shown as spheres and the RNA is shown as sticks. Four of the MSI1-RBD1 RNA binding residues (F23, W29, F65 and K93) that undergo significant peak shifts are highlighted in yellow. C. (Left) Overlay of 2D-HSQC spectra sections of 15N-MSI1-RBD1 (black) titrated with (−)-gossypol. RNA binding residues (highlighted in box) undergo significant line broadening upon addition of (−)-gossypol indicating micro molar affinity between (−)-gossypol and RBD1. The residues that undergo line broadening in RBD1 indicates either they are directly involved in binding, or they are in close proximity of the binding site, or they result from some allosteric effect. (Right) Computational model of the partially hydrated aldehyde form of (−)-gossypol bound to RBD1. The (−)-gossypol is shown in sticks and the protein is represented as in 2B.

DLD-1 cell (data not shown), indication of apoptosis. Curiously, these increases did not correlate well with cell death; (–)-gossypol induced moderate cell death (<10%) in the colon cancer cell lines tested (Figure 4C). By comparison, (–)-gossypol induced nearly 40% increase in cell death in prostate cancer cell lines (Lian et al., 2011), which according to the Oncomine™ database have low MSI1 expression levels. (–)-Gossypol also induced LC3 conversion (Figure 4A, D),

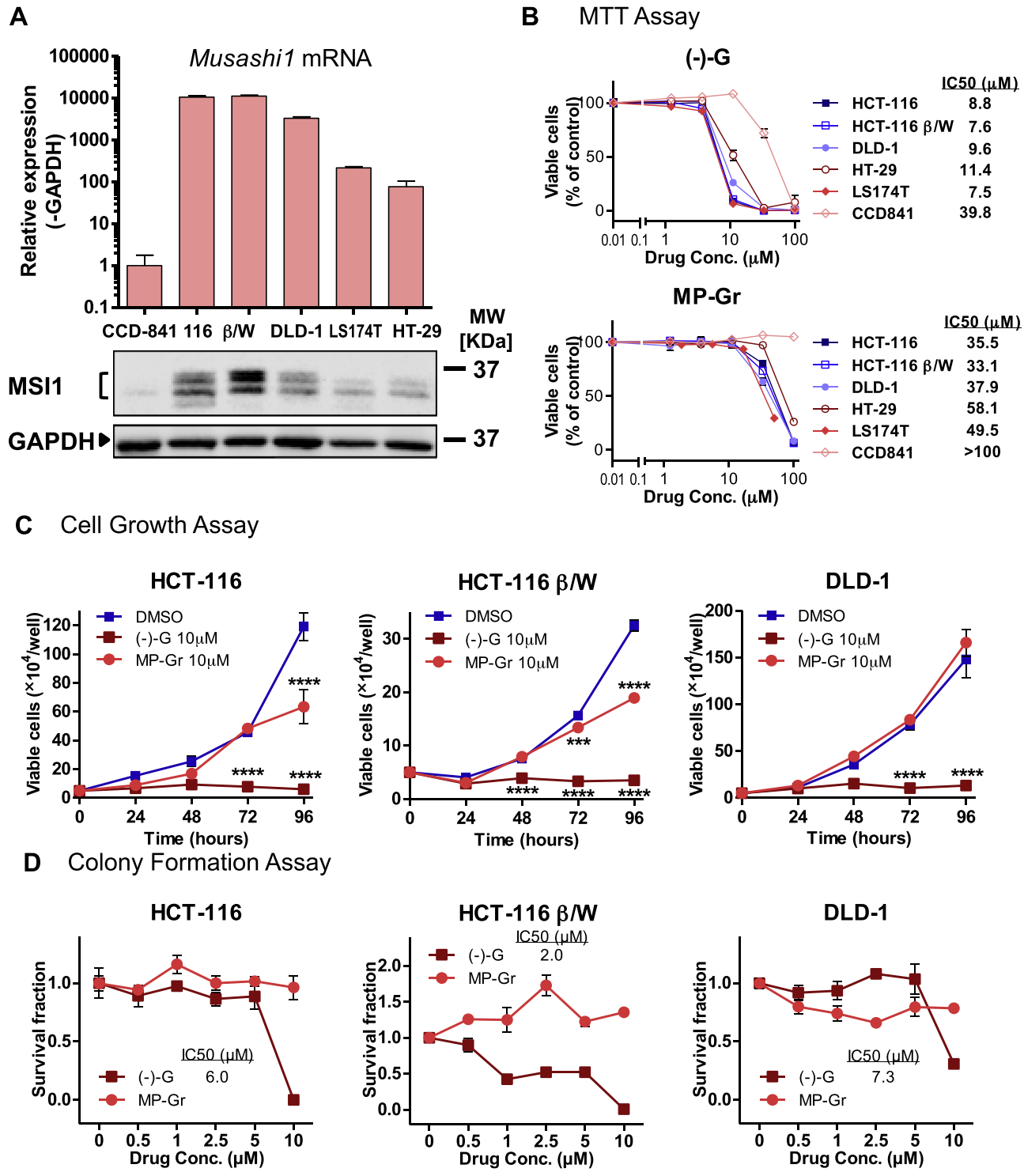

Figure 3 – (−)-Gossypol inhibits colon cancer cell proliferation. A. MSI1 is overexpressed in colon cancer cell lines. B. MTT-based cytotoxicity assay of (−)-gossypol and MP-Gr in selected colon cancer cell lines and in CCD-841, human colon epithelial. (n = 3, one representative experiment of three is shown.) C. (−)-Gossypol inhibits HCT-116, HCT-116 β/W and DLD-1 cell growth. (n = 3, **, $P < 0.01$; ***, $P < 0.001$; ****, $P < 0.0001$ versus DMSO control. One representative experiment of three is shown.) D. Colony formation assay with different doses of (−)-gossypol and MP-Gr in HCT-116, HCT-116 β/W and DLD-1 cells (n = 3, *, $P < 0.05$; **, $P < 0.01$; ****, $P < 0.0001$ versus DMSO control (Concentration 0). One representative experiment of three is shown).

indicating autophagy induction. To investigate the autophagic flux level, we used Bafilomycin A1, which blocks the fusion of autophagosome and lysosome, together with (−)-gossypol. Our data showed that (−)-gossypol induced efficient autophagic flux as evident by the increase of LC3II level and the decrease of P62 degradation in the presence of Bafilomycin A1 (Figure 4D). Taken together, these data indicate that in MSI1-overexpressing colon cancer cells,

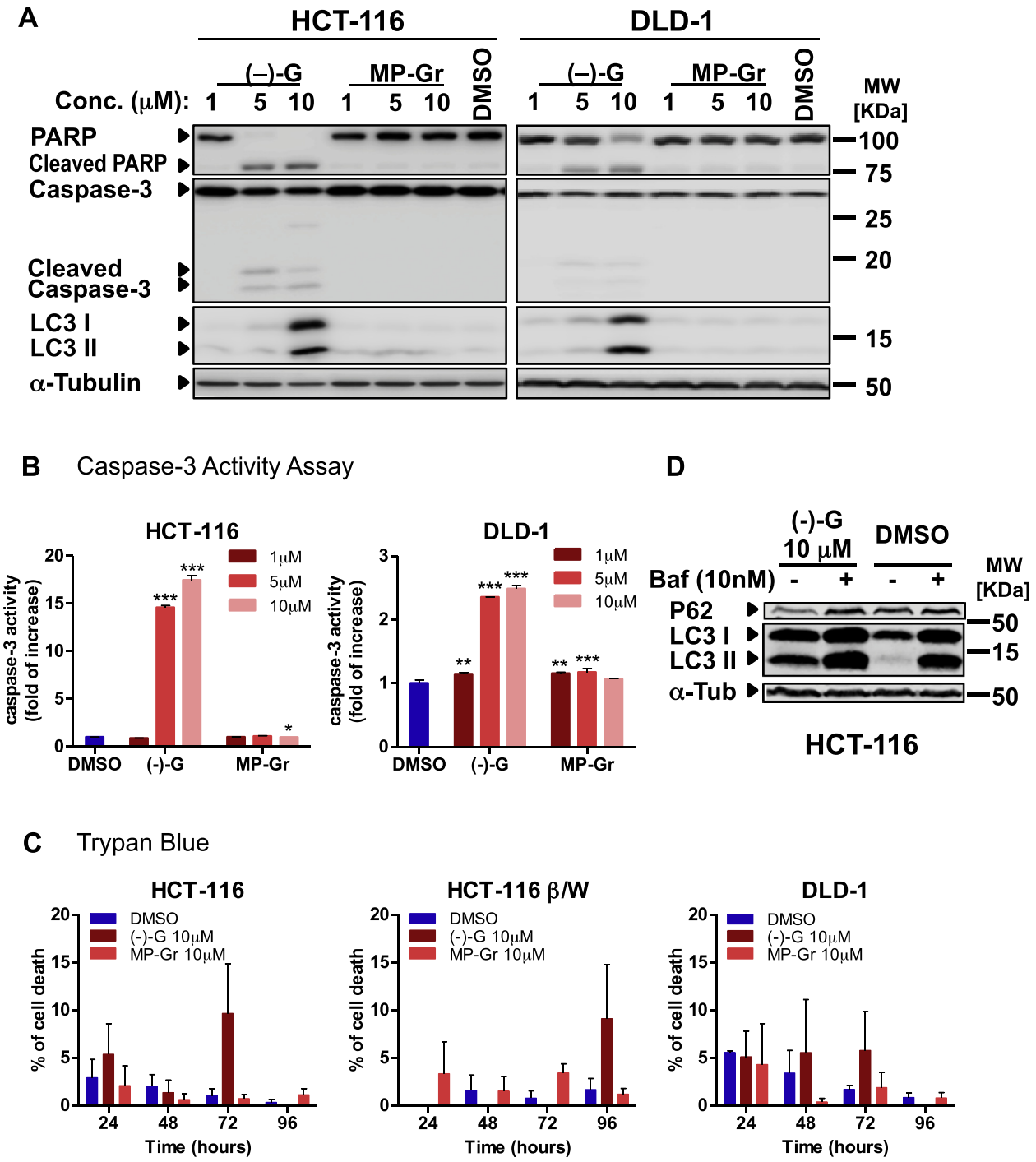

Figure 4 – (−)-Gossypol induces apoptosis and autophagy in colon cancer cell lines. A. Caspapse-3/PARP cleavage and LC3 conversion were observed in colon cancer cell lines treated with different doses of test compounds or DMSO only for 48 h, cell lysate was subject to western blotting for PARP cleavage, caspase-3 cleavage and LC3 I/LC3II expression. B. Dose-dependent increase in caspase-3 activity was observed in (−)-gossypol treated cells. (n = 2) C. Percent of cell death upon drug treatment in different colon cancer cell lines. (n = 3, $P > 0.05$, one representative experiment of three is shown.) D. HCT-116 cells were treated with (−)-gossypol (10 μM) or DMSO, in the presence or absence of Bafilimycin A1 (10 nM). Cell lysates were prepared after 18 h and subjected to immunoblot analysis. All figures, *, $P < 0.05$; **, $P < 0.01$; ***, $P < 0.001$; ****, $P < 0.0001$ versus DMSO control.

(–)-gossypol has a greater effect on cell proliferation through Wnt pathway (see below) relative to its ability to induce cell death, which is consistent with the hypothesis that (–)-gossypol is exerting its effects through MSI1 inhibition. However, in low MSI1/high BCL-2 prostate cancer cells (Lian et al., 2011), (–)-gossypol has a greater effect on apoptosis, presumably through its action as a BCL-2 inhibitor.

3.4. (−)-Gossypol inhibits cell proliferation through MSI1 downstream targets

Our *in vitro* binding and NMR studies above indicate that (−)-gossypol inhibits MSI1-RNA interaction. This inhibition leads to increased Numb and APC expression which results in decreased Notch and Wnt signaling (Moon and Miller, 1997; Pece et al., 2004). Accordingly, we examined the MSI1 downstream signaling pathways after (−)-gossypol treatment in HCT-116 and DLD-1 cells. Figure 5A–B show the reduced expression of activated Notch and several downstream Notch target genes, *HES1*, *c-MYC*, *CYCLIN D1* (*CCND1*) and *SURVIVIN* following treatment with (−)-gossypol but not the negative analog MP-Gr. The protein level of NOTCH1 intracellular domain (NICD) is 12% less in HCT-116 cells treated with 10 μM (−)-gossypol compared to DMSO. In DLD-1 cells, when compared to the DMSO treated sample, 10 μM (−)-gossypol treatment resulted in a 26% reduction of c-MYC protein. Reduction of NICD is not obvious in DLD-1cells treated with 10 μM (−)-gossypol compared to DMSO, however, there is a 30% reduction when we compared 10 μM (−)-gossypol treatment to the negative compound MP-Gr. Down-regulation of *SURVIVIN* was particularly striking, where levels following (−)-gossypol treatment were comparable to that treated with YM155, a known SURVIVIN inhibitor that acts downstream of Notch activation (Cheng et al., 2012) (Figure 5C). Our data also demonstrates (−)-gossypol inhibition of Wnt/Notch signaling genes, *c-MYC* and *CYCLIN D1*. Additional evidence that (−)-gossypol inhibits Wnt signaling comes from quantitative PCR analyses, which showed reduction in *AXIN2* mRNA levels in colon cancer lines following (−)-gossypol treatment (Figure 5B). In a functional Wnt reporter assay performed in HCT-116 cells, (−)-gossypol decreased TOP/FOP reporter signal in a dose-dependent manner (Figure 5D). Figure 5A, B also show (−)-gossypol dose-dependently down-regulated the MSI1 expression. Our previous study (Spears and Neufeld, 2011) and others (Rezza et al., 2010) showed that MSI1 is a Wnt target, and there is a positive feedback loop between MSI1 and Wnt (Rezza et al., 2010). The down-regulation of MSI1 is a consequence of decreased Wnt signaling. (−)-Gossypol treatment also led to the increase of NUMB and P21 protein levels (Figure 5A). When HCT-116 and DLD-1 cells were treated with 10 μM (−)-gossypol, NUMB protein was increased to 110% (HCT-116) and 119% (DLD-1) as compared to DMSO control. *NUMB* and *P21* mRNAs are direct binding and translational repression targets of MSI1 (Battelli et al., 2006; Imai et al., 2001), thus their increases in protein levels are good indications of the MSI1 inhibition. Moreover, we detected increased mRNA levels of *NUMB* and *P21* (Figure 5B). As (−)-gossypol has been reported (Keshmiri-Neghab and Goliaei, 2014; Lian et al., 2011; Meng et al., 2008; Mohammad et al., 2005; Paoluzzi et al., 2008; Zhang et al., 2003, 2010) and in clinical trials (e.g., NCT00286806, NCT00286793, NCT00666666) for targeting Bcl-2 family members, we believe such increase could be non-MSI1 related. Additionally, we see some effect of MP-Gr on the protein and mRNA levels of several genes, consistent with the growth inhibitions observed on HCT-116 and DLD-1 cells, such effect could be due to non-specific targets. Taken together, (−)-gossypol inhibits both Wnt and Notch signaling pathways.

3.5. (−)-Gossypol inhibits HCT-116 xenograft tumor growth

We and others have shown that (−)-gossypol inhibits the growth of multiple human cancers in xenograft mouse models (Coyle et al., 1994; Ko et al., 2007; Lian et al., 2011; Meng et al., 2008; Paoluzzi et al., 2008; Wolter et al., 2006; Zhang et al., 2010). We used a similar assay to determine if (−)-gossypol inhibits the growth of human colon cancer cells with high MSI1 *in vivo*. As shown in Figure 6A, daily oral administration of (−)-gossypol inhibited the growth of human colon cancer HCT-116 xenografts, as compared to the untreated control carboxymethyl cellulose (CMC) ($P < 0.001$, $n = 10$). Western blotting using tumor tissue lysates show that MSI1, together with the activated NOTCH1, CYCLIN D1 and SURVIVIN protein levels were decreased in (−)-gossypol treatment group as compared to CMC control (Figure 6B). Based on the bands' densities, MSI1 protein was down-regulated 39%, the activated NOTCH1 (NICD) 20%, and CYCLIN D1 23%, in the (−)-gossypol-treated tumor versus CMC control. As shown the lower panel of Figure 6B, SURVIVIN protein was down-regulated 55% and 43% in the two (−)-gossypol-treated tumors, as compared with CMC control. These data indicate that (−)-gossypol inhibited MSI1-Wnt/Notch signaling in HCT-116 xenograft tumors *in vivo*, consistent with our *in vitro* data. We also observed increased Caspase-3 activation in the (−)-gossypol-treated tumor sample as indicated by the increased cleaved Caspase-3 level (2.52 fold as compared to CMC control) (Figure 6B). These data indicate that (−)-gossypol promotes apoptosis in the treated tumor tissues, consistent with a previous report in xenograft model of head and neck squamous cell carcinoma (Wolter et al., 2006) and a prostate cancer xenograft model (Meng et al., 2008). The animal body weight of the control and (−)-gossypol-treated mice did not differ significantly throughout the experiment (Figure 6C), suggesting safe oral administration of (−)-gossypol. Our data demonstrate that (−)-gossypol as a single-agent oral therapy is effective *in vivo* in inhibiting tumor growth of human colon cancers with high levels of MSI1.

4. Discussion

In this study, we report that (−)-gossypol is a potent inhibitor of MSI1-*Numb* RNA interaction as determined by FP-based screening. We validated direct binding of (−)-gossypol to the RBD1 of MSI1 protein using SPR and NMR, and carried out *in silico* docking studies to suggest a possible binding mode for the compound. Further studies showed that (−)-gossypol inhibits colon cancer cell proliferation and down-regulates both Notch and Wnt signaling pathways. Using a colon cancer xenograft model, we demonstrated that (−)-gossypol inhibits tumor growth as a single agent.

MSI1 is an RNA binding protein thought to act as a cancer maintenance factor through its ability to repress NUMB, APC

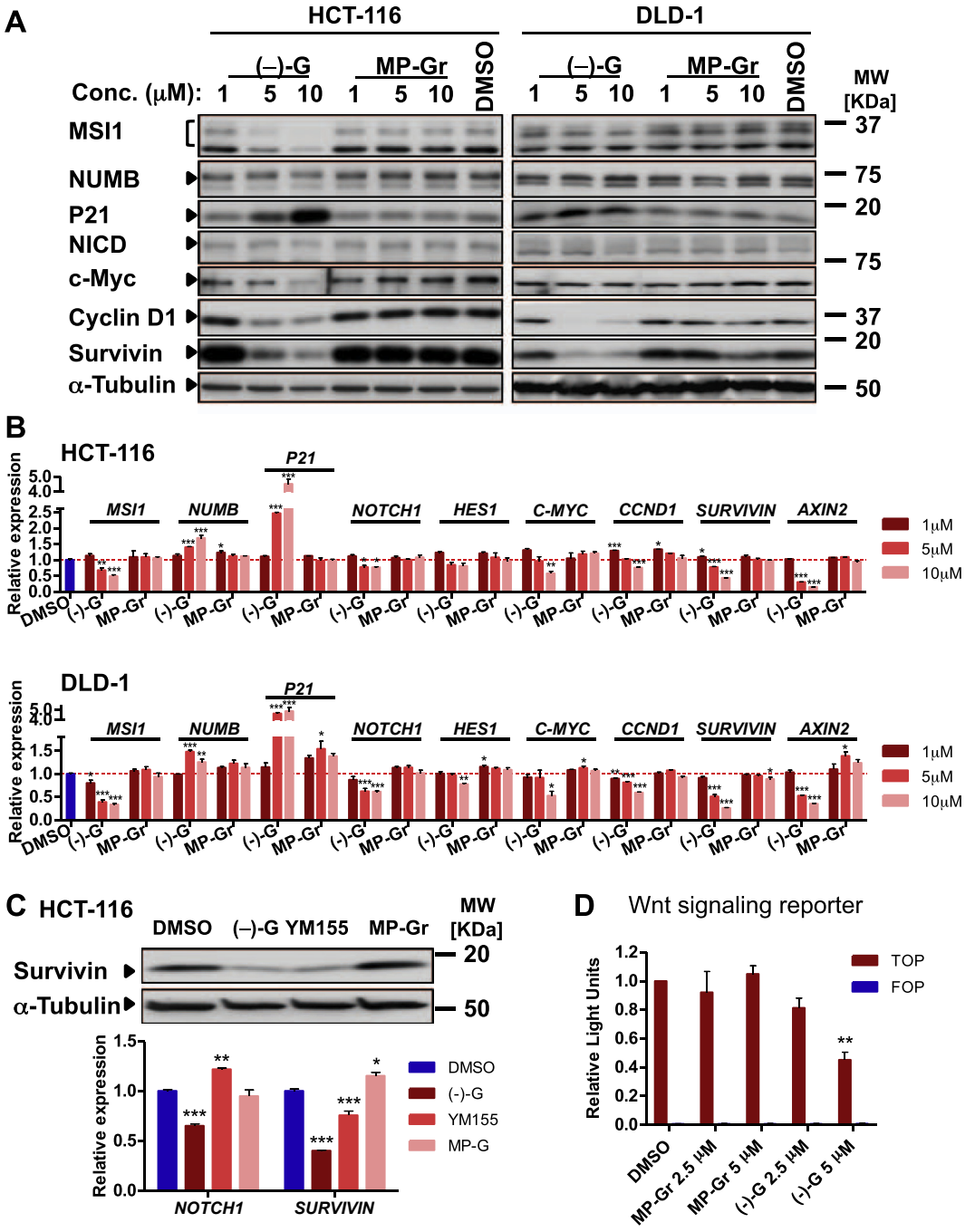

Figure 5 – (−)-Gossypol down-regulates Notch/Wnt signaling in colon cancer cell lines. Notch/Wnt target genes expression changes upon drug treatment were examined in HCT-116 and DLD-1 cells by western blotting (A) and by quantitative real-time PCR (B) with indicated doses. Cells were collected 48 h (western) or 24 h (real-time PCR) after drug treatment. NICD: NOTCH1 intracellular domain; CCND1: CYCLIN D1. C. Confirmation of SURVIVIN knockdown compared to YM155, a SURVIVIN inhibitor. Cells were collected 48 h after treatment. Dose: (−)-gossypol and MP-Gr: 10 μM; YM155: 10 nM. D. (−)-Gossypol inhibits Wnt/β-catenin signaling reporter. HCT-116 cells were transfected with Top or Fop Flash reporter constructs. Cells were treated with compounds for 24 h in the presence of 20 mM LiCl. All figures, n = 3; *, $P < 0.05$; **, $P < 0.01$; ***, $P < 0.001$ versus DMSO control.

and P21 expression, which results in increased Notch and Wnt signaling. We used an FP assay to screen compounds for their ability to inhibit the RNA binding activity of MSI1. Our NMR studies indicate that (–)-gossypol competes with target RNAs for binding to MSI1. (–)-Gossypol induced the residue shifts in the RNA-binding pocket of MSI1 RBD1, including residues F23, K93, F65 that form stacking interactions with cognate RNA. Structure-based modeling suggests that (–)-gossypol may mimic these stacking interactions when binding to this pocket. The observed shift at W29 in the upper

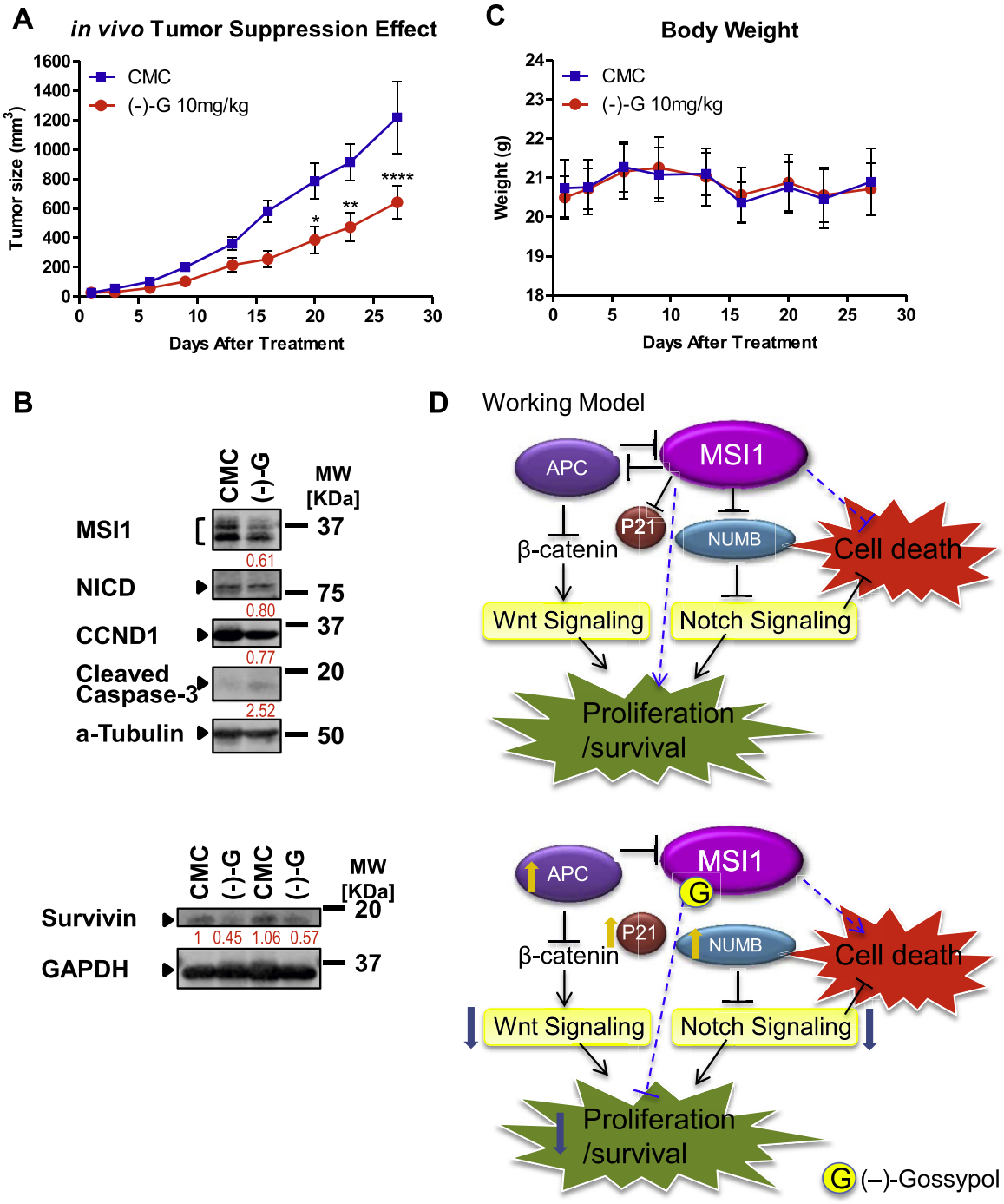

Figure 6 – Oral administration of (−)-gossypol inhibited HCT-116 xenograft growth. A. (−)-Gossypol potently inhibited the HCT-116 xenograft tumor growth in nude mice as a single-agent oral therapy. The data shown are average tumor size (means ± S.E.M., n = 10) versus vehicle control carboxymethyl cellulose (CMC) (n = 10). *, $P < 0.05$; **, $P < 0.01$; ****, $P < 0.0001$. B. (−)-Gossypol down-regulated Wnt/Notch signaling and induced apoptosis in HCT-116 xenograft model. Lysates from HCT-116 xenograft tumor tissues treated with vehicle (CMC) or (−)-gossypol for one week and blotted for MSI1, NICD, CCND1, SURVIVIN and Cleaved Caspase-3. Relative band intensities were indicated underneath the bands for (−)-gossypol treated tumor samples. NICD: NOTCH1 intracellular domain; CCND1: CYCLIN D1. C. Body weight change during the course of treatment. D. Working model: (Up) In cells with MSI1 overexpression, MSI1 blocks the translation of *NUMB* and *APC* mRNA, which leads to the up-regulation of Notch/Wnt signaling. Thus MSI1 indirectly promotes proliferation/survival of the cells and inhibits cell death; (Down) In the presence of (−)-gossypol, (−)-gossypol binds to the RBD1 of MSI1, presumably releasing *NUMB*, *APC* and *P21* mRNA from their translational repression. Increased level of Numb and APC protein will block Notch and Wnt signaling respectively. Increased P21 will block cell cycle progression. Thus (−)-gossypol-MSI1 complex indirectly blocks proliferation/survival of the cells.

portion of the binding pocket could be due to a second, cryptic (–)-gossypol binding site or an allosteric effect of binding to the lower portion of the pocket. Additional biochemical studies and X-ray crystallography will distinguish between these two possibilities. So far, there are no reported small molecule inhibitors of the RNA-binding protein MSI1, potentially due to lacking of well-defined pocket in RNA binding domain.

Further investigation of (–)-gossypol functions showed that (–)-gossypol inhibits cell proliferation, induces apoptosis and autophagy, and represses Notch/Wnt signaling in colon cancer cell lines with MSI1 overexpression; (–)-gossypol also inhibits colon cancer xenograft tumor growth *in vivo*. Our previous study has shown that (–)-gossypol induces apoptosis and autophagy in prostate cancer cell lines (Lian et al., 2011), but does not correlate (–)-gossypol with MSI1 expression level or Wnt signaling, because Wnt signaling is not a major pathway in the initiation and progression of prostate cancers. In colon cancers, however, Wnt signaling played a major role in the tumor initiation and progression. Our working model in Figure 6D shows that in cells with MSI1 overexpression, MSI1 blocks the translation of *NUMB* and *APC* mRNA, which leads to the up-regulation of both Notch and Wnt signaling pathways. Thus MSI1 indirectly promotes proliferation/survival of the cells and inhibits cell death; (–)-gossypol binds to the RBD1 of MSI1, presumably releasing *NUMB*, *APC* and *P21* mRNA from their translational repression. Increased level of NUMB and APC protein will block Notch and Wnt signaling, respectively. Increased P21 and decreased CYCLIN D1 will block cell cycle progression, which is consistent with cell cycle arrest observed in (–)-gossypol-treated HT-29 cells (Zhang et al., 2003). Autophagy is another way to promote cell cycle arrest, as it drives cells into quiescence. We conclude that (–)-gossypol induces autophagy in colon cancer cells, and such induction puts cells into a cytostatic state with G0/G1 arrest (data not shown and ref. (Zhang et al., 2003)); Simultaneously, (–)-gossypol blockade of the MSI1-RNA interaction leads to down regulation of Notch and Wnt signaling, thus blocking proliferation/survival (Figure 6D).

While (–)-gossypol shows strong binding to the newly identified target MSI1 with promising *in vitro* activity, it is not a specific MSI1 inhibitor as it also binds to many other targets. For example, (–)-gossypol has been shown to bind to BCL-2 family of proteins and inhibit their anti-apoptotic and/or anti-autophagic function in various cancer cells and to inhibit tumor growth *in vivo* (Lian et al., 2011; Meng et al., 2008; Oliver et al., 2004; Paoluzzi et al., 2008). Our current study identified a new target of (–)-gossypol, and validated its function in inhibiting Notch and Wnt signaling through MSI1 inhibition. (–)-Gossypol binds to MSI1 with a similar or even higher affinity than it binds to Bcl-2 family members, raising the possibility that the drug may also have utility in the treatment of cancers associated with high levels of MSI1 expression and Notch/Wnt signaling. Our future efforts will focus on further examining this novel mechanism of (–)-gossypol. Since the drug already shows promise in advanced clinical trials, such efforts may well lead to a new approach to cancer chemotherapy.

Grant support

This study was supported in part by National Institutes of Health grant R01 CA178831 (to L. X., K. N., J. A.), K-INBRE (P20 GM103418) Bridging Grant; Kansas Bioscience Authority Rising Star Award, and University of Kansas Cancer Center Pilot Grant (to L. X.); NIH COBRE at KU CCET Pilot Project (P30 RR030926 to K. N.), NIH R01 AI074856 (to R. N. D.), and the University of Kansas Bold Aspiration Strategic Initiative Award (to L. X. and K. N.). The sponsors had no role in the study design, in the collection, analysis, and interpretation of data.

Disclosure of potential conflicts of interest

The authors declare no competing interest.

Acknowledgments

We thank S. Jimmy Budiardjo and Na Zhang for their help with GST-MSI1 protein production, Annemarie Chilton for providing GB1-RBD1 protein, and Heather Shinogle for help with the cell cycle analysis. We are grateful to OpenEye Scientific Software (Santa Fe, NM) for providing an academic license for the use of OMEGA, ROCS, MolProp, and QuacPac. We thank the NCI/DTP Open Chemical Repository (http://dtp.cancer.gov) for providing the compound libraries.

Appendix A. Supplementary data

Supplementary data related to this article can be found at http://dx.doi.org/10.1016/j.molonc.2015.03.014.

REFERENCES

Aviv, T., Lin, Z., Lau, S., Rendl, L.M., Sicheri, F., Smibert, C.A., 2003. The RNA-binding SAM domain of Smaug defines a new family of post-transcriptional regulators. Nat. Struct. Biol. 10, 614–621.

Battelli, C., Nikopoulos, G.N., Mitchell, J.G., Verdi, J.M., 2006. The RNA-binding protein Musashi-1 regulates neural development through the translational repression of p21WAF-1. Mol. Cell. Neurosci. 31, 85–96.

Chan, T.A., Wang, Z., Dang, L.H., Vogelstein, B., Kinzler, K.W., 2002. Targeted inactivation of CTNNB1 reveals unexpected effects of beta-catenin mutation. Proc. Natl. Acad. Sci. USA 99, 8265–8270.

Charlesworth, A., Wilczynska, A., Thampi, P., Cox, L.L., MacNicol, A.M., 2006. Musashi regulates the temporal order of mRNA translation during Xenopus oocyte maturation. EMBO J. 25, 2792–2801.

Cheng, Q., Ling, X., Haller, A., Nakahara, T., Yamanaka, K., Kita, A., Koutoku, H., Takeuchi, M., Brattain, M.G., Li, F., 2012. Suppression of survivin promoter activity by YM155 involves disruption of Sp1-DNA interaction in the

survivin core promoter. Int. J. Biochem. Mol. Biol. 3, 179–197.
Clingman, C.C., Deveau, L.M., Hay, S.A., Genga, R.M., Shandilya, S.M., Massi, F., Ryder, S.P., 2014. Allosteric inhibition of a stem cell RNA-binding protein by an intermediary metabolite. eLife 3.
Coyle, T., Levante, S., Shetler, M., Winfield, J., 1994. In vitro and in vivo cytotoxicity of gossypol against central nervous system tumor cell lines. J. Neurooncol. 19, 25–35.
Frank Delaglio, S.G., Vuister, Geerten W., Zhu, Guang, Pfeifer, John, Bax, Ad, 1995. NMRPipe: a multidimensional spectral processing system based on UNIX pipes. J. Biomol. NMR 6, 277–293.
Estrada, D.F., Boudreaux, D.M., Zhong, D., St Jeor, S.C., De Guzman, R.N., 2009. The hantavirus glycoprotein G1 tail contains dual CCHC-type classical zinc fingers. J. Biol. Chem. 284, 8654–8660.
Fan, L.-F., Dong, W.-G., Jiang, C.-Q., Xia, D., Liao, F., Yu, Q.-F., 2010. Expression of putative stem cell genes Musashi-1 and β1-integrin in human colorectal adenomas and adenocarcinomas. Int. J. Colorectal Dis. 25, 17–23.
Harper, S., Speicher, D.W., 2011. Purification of proteins fused to glutathione S-transferase. Methods Mol. Biol. 681, 259–280.
Imai, T., Tokunaga, A., Yoshida, T., Hashimoto, M., Mikoshiba, K., Weinmaster, G., Nakafuku, M., Okano, H., 2001. The neural RNA-binding protein Musashi1 translationally regulates mammalian numb gene expression by interacting with its mRNA. Mol. Cell. Biol. 21, 3888–3900.
Johnson, B.A., 2004. Using NMRView to visualize and analyze the NMR spectra of macromolecules. In: Downing, A.K. (Ed.), Protein NMR Techniques. Humana Press, pp. 313–352.
Kaneko, Y., Sakakibara, S., Imai, T., Suzuki, A., Nakamura, Y., Sawamoto, K., Ogawa, Y., Toyama, Y., Miyata, T., Okano, H., 2000. Musashi1: an evolutionally conserved marker for CNS progenitor cells including neural stem cells. Dev. Neurosci. 22, 139–153.
Kawahara, H., Okada, Y., Imai, T., Iwanami, A., Mischel, P.S., Okano, H., 2011. Musashi1 cooperates in abnormal cell lineage protein 28 (Lin28)-mediated let-7 family microRNA biogenesis in early neural differentiation. J. Biol. Chem. 286, 16121–16130.
Keshmiri-Neghab, H., Goliaei, B., 2014. Therapeutic potential of gossypol: an overview. Pharm. Biol. 52, 124–128.
Ko, C.H., Shen, S.C., Yang, L.Y., Lin, C.W., Chen, Y.C., 2007. Gossypol reduction of tumor growth through ROS-dependent mitochondria pathway in human colorectal carcinoma cells. Int. J. Cancer 121, 1670–1679.
Kuwako, K., Kakumoto, K., Imai, T., Igarashi, M., Hamakubo, T., Sakakibara, S., Tessier-Lavigne, M., Okano, H.J., Okano, H., 2010. Neural RNA-binding protein Musashi1 controls midline crossing of precerebellar neurons through posttranscriptional regulation of Robo3/Rig-1 expression. Neuron 67, 407–421.
Li, D., Peng, X., Yan, D., Tang, H., Huang, F., Yang, Y., Peng, Z., 2011. Msi-1 is a predictor of survival and a novel therapeutic target in colon cancer. Ann. Surg. Oncol. 18, 2074–2083.
Li, L., Hao, X., Qin, J., Tang, W., He, F., Smith, A., Zhang, M., Simeone, D.M., Qiao, X.T., Chen, Z.N., Lawrence, T.S., Xu, L., 2014. Antibody against CD44s inhibits pancreatic tumor initiation and post-radiation recurrence in mice. Gastroenterology.
Li, L., Tang, W., Wu, X., Karnak, D., Meng, X., Thompson, R., Hao, X., Li, Y., Qiao, X.T., Lin, J., Fuchs, J., Simeone, D.M., Chen, Z.N., Lawrence, T.S., Xu, L., 2013. HAb18G/CD147 promotes pSTAT3-mediated pancreatic cancer development via CD44s. Clin. Cancer Res. 19, 6703–6715.
Lian, J., Wu, X., He, F., Karnak, D., Tang, W., Meng, Y., Xiang, D., Ji, M., Lawrence, T.S., Xu, L., 2011. A natural BH3 mimetic induces autophagy in apoptosis-resistant prostate cancer via modulating Bcl-2-Beclin1 interaction at endoplasmic reticulum. Cell Death Differ. 18, 60–71.
Ma, Y.-H., Mentlein, R., Knerlich, F., Kruse, M.-L., Mehdorn, H., Held-Feindt, J., 2008. Expression of stem cell markers in human astrocytomas of different WHO grades. J. Neuro-Oncology 86, 31–45.
Meng, Y., Tang, W., Dai, Y., Wu, X., Liu, M., Ji, Q., Ji, M., Pienta, K., Lawrence, T., Xu, L., 2008. Natural BH3 mimetic (-)-gossypol chemosensitizes human prostate cancer via Bcl-xL inhibition accompanied by increase of Puma and Noxa. Mol. Cancer Ther. 7, 2192–2202.
Minuesa, G., Antczak, C., Shum, D., Radu, C., Bhinder, B., Li, Y., Djaballah, H., Kharas, M.G., 2014. A 1536-well fluorescence polarization assay to screen for modulators of the MUSASHI family of RNA-binding proteins. Comb. Chem. High Throughput Screen. 17, 596–609.
Miyanoiri, Y., Kobayashi, H., Imai, T., Watanabe, M., Nagata, T., Uesugi, S., Okano, H., Katahira, M., 2003. Origin of higher affinity to RNA of the N-terminal RNA-binding domain than that of the C-terminal one of a mouse neural protein, Musashi1, as revealed by comparison of their structures, modes of interaction, surface electrostatic potentials, and backbone dynamics. J. Biol. Chem. 278, 41309–41315.
Mohammad, R.M., Wang, S., Banerjee, S., Wu, X., Chen, J., Sarkar, F.H., 2005. Nonpeptidic small-molecule inhibitor of Bcl-2 and Bcl-XL, (-)-Gossypol, enhances biological effect of genistein against BxPC-3 human pancreatic cancer cell line. Pancreas 31, 317–324.
Moon, R.T., Miller, J.R., 1997. The APC tumor suppressor protein in development and cancer. Trends Genet. 13, 256–258.
Morris, G.M., Huey, R., Lindstrom, W., Sanner, M.F., Belew, R.K., Goodsell, D.S., Olson, A.J., 2009. AutoDock4 and AutoDockTools4: Automated docking with selective receptor flexibility. J. Comput. Chem. 30, 2785–2791.
Nakamura, M., Okano, H., Blendy, J.A., Montell, C., 1994. Musashi, a neural RNA-binding protein required for Drosophila adult external sensory organ development. Neuron 13, 67–81.
O'Boyle, N.M., Banck, M., James, C.A., Morley, C., Vandermeersch, T., Hutchison, G.R., 2011. Open Babel: an open chemical toolbox. J. Cheminform 3, 33.
Ohyama, T., Nagata, T., Tsuda, K., Kobayashi, N., Imai, T., Okano, H., Yamazaki, T., Katahira, M., 2012. Structure of Musashi1 in a complex with target RNA: the role of aromatic stacking interactions. Nucleic Acids Res. 40, 3218–3231.
Okano, H., Kawahara, H., Toriya, M., Nakao, K., Shibata, S., Imai, T., 2005. Function of RNA-binding protein Musashi-1 in stem cells. Exp. Cell Res. 306, 349–356.
Oliver, C.L., Bauer, J.A., Wolter, K.G., Ubell, M.L., Narayan, A., O'Connell, K.M., Fisher, S.G., Wang, S., Wu, X., Ji, M., Carey, T.E., Bradford, C.R., 2004. In vitro effects of the BH3 mimetic, (-)-gossypol, on head and neck squamous cell carcinoma cells. Clin. Cancer Res. 10, 7757–7763.
Pagano, J.M., Clingman, C.C., Ryder, S.P., 2011. Quantitative approaches to monitor protein-nucleic acid interactions using fluorescent probes. RNA 17, 14–20.
Paoluzzi, L., Gonen, M., Gardner, J.R., Mastrella, J., Yang, D., Holmlund, J., Sorensen, M., Leopold, L., Manova, K., Marcucci, G., Heaney, M.L., O'Connor, O.A., 2008. Targeting Bcl-2 family members with the BH3 mimetic AT-101 markedly enhances the therapeutic effects of chemotherapeutic agents in in vitro and in vivo models of B-cell lymphoma. Blood 111, 5350–5358.
Pece, S., Serresi, M., Santolini, E., Capra, M., Hulleman, E., Galimberti, V., Zurrida, S., Maisonneuve, P., Viale, G., Di Fiore, P.P., 2004. Loss of negative regulation by Numb over Notch is relevant to human breast carcinogenesis. J. Cell. Biol. 167, 215–221.

Potten, C.S., Booth, C., Tudor, G.L., Booth, D., Brady, G., Hurley, P., Ashton, G., Clarke, R., Sakakibara, S., Okano, H., 2003. Identification of a putative intestinal stem cell and early lineage marker; musashi-1. Differentiation 71, 28–41.

Rezza, A., Skah, S., Roche, C., Nadjar, J., Samarut, J., Plateroti, M., 2010. The overexpression of the putative gut stem cell marker Musashi-1 induces tumorigenesis through Wnt and Notch activation. J. Cell. Sci. 123, 3256–3265.

Sakakibara, S., Imai, T., Hamaguchi, K., Okabe, M., Aruga, J., Nakajima, K., Yasutomi, D., Nagata, T., Kurihara, Y., Uesugi, S., Miyata, T., Ogawa, M., Mikoshiba, K., Okano, H., 1996. Mouse-Musashi-1, a neural RNA-binding protein highly enriched in the mammalian CNS stem cell. Dev. Biol. 176, 230–242.

Seigel, G.M., Hackam, A., Ganguly, A., Mandell, L., Gonzalez-Fernandez, F., 2007. Human embryonic and neuronal stem cell markers in retinoblastoma. Mol. Vis. 13, 823–832.

Shaomeng Wang, Yang D., Liang Xu, 2012. Small molecule antagonists of Bcl-2 family proteins. (US patent 8163805 B2).

Siddall, N.A., McLaughlin, E.A., Marriner, N.L., Hime, G.R., 2006. The RNA-binding protein Musashi is required intrinsically to maintain stem cell identity. Proc. Natl. Acad. Sci. USA 103, 8402–8407.

Spears, E., Neufeld, K.L., 2011. Novel double-negative feedback loop links Adenomatous polyposis coli and Musashi in colon epithelia. J. Biol. Chem. 286, 4946–4950.

Sugiyama-Nakagiri, Y., Akiyama, M., Shibata, S., Okano, H., Shimizu, H., 2006. Expression of RNA-binding protein Musashi in hair follicle development and hair cycle progression. Am. J. Pathol. 168, 80–92.

Sureban, S.M., May, R., George, R.J., Dieckgraefe, B.K., McLeod, H.L., Ramalingam, S., Bishnupuri, K.S., Natarajan, G., Anant, S., Houchen, C.W., 2008. Knockdown of RNA binding protein Musashi-1 leads to tumor regression in vivo. Gastroenterology 134, 1448–1458 e1442.

Takahashi, T., Suzuki, H., Imai, T., Shibata, S., Tabuchi, Y., Tsuchimoto, K., Okano, H., Hibi, T., 2013. Musashi-1 post-transcriptionally enhances phosphotyrosine-binding domain-containing m-Numb protein expression in regenerating gastric mucosa. PLoS One 8, e53540.

Toda, M., Iizuka, Y., Yu, W., Imai, T., Ikeda, E., Yoshida, K., Kawase, T., Kawakami, Y., Okano, H., Uyemura, K., 2001. Expression of the neural RNA-binding protein Musashi1 in human gliomas. Glia 34, 1–7.

Wang, X.-Y., Penalva, L., Yuan, H., Linnoila, R.I., Lu, J., Okano, H., Glazer, R., 2010. Musashi1 regulates breast tumor cell proliferation and is a prognostic indicator of poor survival. Mol. Cancer 9, 221.

Wolter, K.G., Wang, S.J., Henson, B.S., Wang, S., Griffith, K.A., Kumar, B., Chen, J., Carey, T.E., Bradford, C.R., D'Silva, N.J., 2006. (-)-gossypol inhibits growth and promotes apoptosis of human head and neck squamous cell carcinoma in vivo. Neoplasia 8, 163–172.

Wu, X., Li, M., Qu, Y., Tang, W., Zheng, Y., Lian, J., Ji, M., Xu, L., 2010. Design and synthesis of novel Gefitinib analogues with improved anti-tumor activity. Bioorg. Med. Chem. 18, 3812–3822.

Ye, F., Zhou, C., Cheng, Q., Shen, J., Chen, H., 2008. Stem-cell-abundant proteins Nanog, Nucleostemin and Musashi1 are highly expressed in malignant cervical epithelial cells. BMC Cancer 8, 108.

Yokota, N., Mainprize, T.G., Taylor, M.D., Kohata, T., Loreto, M., Ueda, S., Dura, W., Grajkowska, W., Kuo, J.S., Rutka, J.T., 2004. Identification of differentially expressed and developmentally regulated genes in medulloblastoma using suppression subtraction hybridization. Oncogene 23, 3444–3453.

Zhang, M., Liu, H., Guo, R., Ling, Y., Wu, X., Li, B., Roller, P.P., Wang, S., Yang, D., 2003. Molecular mechanism of gossypol-induced cell growth inhibition and cell death of HT-29 human colon carcinoma cells. Biochem. Pharmacol. 66, 93–103.

Zhang, X.Q., Huang, X.F., Mu, S.J., An, Q.X., Xia, A.J., Chen, R., Wu, D.C., 2010. Inhibition of proliferation of prostate cancer cell line, PC-3, in vitro and in vivo using (-)-gossypol. Asian J. Androl. 12, 390–399.